

# Assessment of a Quasi-Optimum Very Low Complexity CPM Receiver over Flat Rayleigh Fading

Francisco A. Monteiro<sup>(1)</sup>, António J. Rodrigues<sup>(1,2)</sup>

(1) Instituto de Telecomunicações; (2) Instituto Superior Técnico, Technical University of Lisbon

Lisbon, Portugal

E-mail: frmo@lx.it.pt

**Abstract**—This paper proposes the use of a new family of receivers for continuous phase modulation (CPM) having very small complexity, operating with both elementary hardware and simple numeric processing. It results from an intervention on the optimum receiver for signals corrupted by additive white gaussian noise (AWGN) on three stages of the process: replacement of the bank of filters by projection on Walsh functions; derivation of metrics from 1/4 of them by using a symmetry-based algorithm; and sequence detection with the M-algorithm. This receiver had already proved to be quasi-optimum on pure AWGN case. On this paper the receiver is tested over AWGN and frequency-flat Rayleigh fading (FFRF) with and without phase compensation. It is found that the geometric algorithm used to derive metrics introduces robustness to phase synchronism errors. The research on the reduction limits of the space dimension is conducted using catastrophic  $M$ -ary CPM schemes, taking advantage of their small number of phase states. Performance of 1REC  $h=1/2$  16-ary under Rayleigh fading is for the first time presented. All the outcomes prove to be valid for two proposed CPM schemes of high power gain. Two optimum CPM schemes and their respective sub-optimum receivers for mobile communications are presented. The receiver remains quasi-optimum over the tested multipath channel. The common minimum shift keying (MSK) is a particular case of this research.

## I. INTRODUCTION

Continuous phase modulation (CPM) signals have constant amplitude and so they are a good solution for systems requiring insensitivity to non-linear amplitude amplification. Their phase continuity allows good spectral performance and implies a code gain due to the inherent memory effect. These properties have motivated the common use of GMSK (gaussian minimum shift keying), which is a simple member of the CPM family, in widespread use systems such as GSM/DCS, PCS, DECT, CT2 and Bluetooth. The use of others CPM schemes more spectrally efficient and better power efficient was restrained owing to excessive detection complexity [1]. The number of analogue matched filters (or correlators) needed is often unbearable for practical implementation. The number of phase states to be detected can also be very large. The conception of simple receivers is nowadays a main concern within CPM research.

### I. CPM FORMATTING AND PERFORMANCE

Every CPM signals can be expressed in the form

$$s(t, \gamma) = \sqrt{2E_s/T_s} \cos(\omega_c t + \varphi(t, \gamma) + \varphi_0). \quad (1)$$

The carrier frequency is  $f_c$ , where  $\omega_c = 2\pi f_c$ ,  $\varphi_0$  is the arbitrary initial phase and  $E_s$  is the energy per symbol, related

with the bit energy by  $E_s = \log_2(M) \cdot E_b$ . Channel symbols are  $\gamma_i \in \{\pm 1, \pm 3, \dots, \pm(M-1)\}$ , forming the  $M$ -ary sequence  $\gamma$ . Each symbol  $\gamma_i$  carries  $\log_2(M)$  bits as a result of a natural mapping of the information bits stream  $\alpha$ . The information carried by  $N_s$  channel symbols is keyed in signal's phase as

$$\varphi(t, \gamma) = 2\pi h \sum_{i=0}^{N_s} \gamma_i q(t - iT_s). \quad (2)$$

A constant modulation index,  $h=p/q$ , is considered, where  $p$  and  $q$  are integers with no common factors. ( $h$  is rational in order to have a finite number of phase states.) Phase transition pulse shape,  $q(t)$ , affects phase transitions shape during  $L$  symbols. However, its effect remains until the end of the transmitted sequence.  $q(t)$  is defined by the frequency pulse

$$g(t): q(t) = \int_{-\infty}^t g(\tau) d\tau. \text{ The normalisation } q(t) = \int_0^{\infty} g(\tau) d\tau =$$

$1/2$  is applied so that the maximum phase transition during a symbol time,  $T_s$ , is  $h \cdot (M-1) \cdot \pi$ . Different frequency pulses define different CPM families. The most common are: LREC, LRC ( $L$  is the variable mentioned above) and GMSK [1,2]. LREC is defined by  $g(t) = \text{rect}[t/(LT_s)]/2$ , where  $\text{rect}(t) = 1$  for  $-1/2 < |t| < 1/2$  and zero elsewhere. Schemes with 1REC pulses are also known as CPFSSK (continuous phase frequency shift keying). A smoother  $g(t)$  can improve the spectral efficiency of schemes with LREC pulses, an example is the referred LRC which has a raised cosine pulse shaping.

In order to evaluate CPM power performance one uses the minimum normalised squared Euclidean distance (MNSD) between two signals transporting sequences  $\gamma$  and  $\gamma'$ :

$$d_{\min}^2(\gamma, \gamma') = 1/(2E_s) \min_{\tau: \gamma \neq \gamma'} \int_0^{\infty} [s(t, \gamma) - s(t, \gamma')]^2 dt. \quad (3)$$

Bit error rate (BER) is given by (e.g. [1])

$$P_b \approx C \cdot Q\left(\sqrt{d_{\min}^2 \frac{E_b}{N_0}}\right) \approx Q\left(\sqrt{d_{\min}^2 \frac{E_b}{N_0}}\right). \quad (4)$$

$C$  is a constant  $\approx 1$ .  $Q(x)$  is the area under the unit variance gaussian distribution in  $[x, \infty]$ . Power efficiency comparisons can be made from (4), defining the gain relative to MSK:

$$G = 10 \cdot \log_{10}(d_{\min}^2 / 2) \text{ [dB]}. \quad (5)$$

Bandwidth is usually given in terms of  $B_\epsilon T_b$  where  $B_\epsilon$  is the bandwidth that encloses  $\epsilon\%$  of transmitted power and  $T_b = T_s / \log(M)$  is the bit interval. The bit rate is  $R_b = 1/T_b$  and the spectrum efficiency is  $\zeta = 1/(B_\epsilon T_b) = R_b/B_\epsilon$ . For MSK  $B_{99,0} T_b = 1.2$ .

We acknowledge the support of FCT under the POSI program sponsored by FEDER.

A lower  $h$  makes phase transitions to become smoother and so it constrains bandwidth, though that makes MNSED to decrease due to the greater similitude among phase transitions during each  $T_s$  interval. A greater  $M$  enhances simultaneously spectrum and power behavior at a cost of complexity increase.

## II. OPTIMUM DETECTION

To obtain metrics for each one of the  $\Xi$  phase transitions the optimum CPM receiver requires  $2\Xi$  matched filters (or equivalent correlators), one for each branch I and Q. Metrics have to be calculated for all transitions  $\tau_{1,b} \in \{\tau_{1,1}, \tau_{1,2}, \dots, \tau_{1,\Xi}\}$  and all  $\tau_{Q,b} \in \{\tau_{Q,1}, \tau_{Q,2}, \dots, \tau_{Q,\Xi}\}$ . Considering  $n(t)$  additive white gaussian noise (AWGN), after baseband conversion one gets the  $y(t)=s(t,\boldsymbol{\gamma})+n(t)$ . I and Q metrics for  $b=1, 2, \dots, \Xi$ , are then

$$\Lambda_i(b) = \int_{T_i} y_{I,i}(t) \tau_{1,b}(t) dt + \int_{T_i} y_{Q,i}(t) \tau_{Q,b}(t) dt = \Lambda_{I,i}(b) + \Lambda_{Q,i}(b). \quad (6)$$

In more detail, for the same  $b$ , the branch metrics are

$$\Lambda_{I,i}(b) = \int_{iT_i}^{(i+1)T_i} y(t) \cdot \cos[2\pi h \gamma_b q(t)] dt \quad (7a)$$

$$\Lambda_{Q,i}(b) = \int_{iT_i}^{(i+1)T_i} y(t) \cdot \sin[2\pi h \gamma_b q(t)] dt. \quad (7b)$$

Finally, having all the metrics, the problem is solved by a maximum likelihood sequence detector (MLSD). The detection complexity of CPM schemes is measured in terms of  $\Xi$  and the total number of states, being that number

$$S = q \cdot M^{L-1}, \quad \text{for even } p \quad (8a)$$

$$S = 2q \cdot M^{L-1}, \quad \text{for odd } p. \quad (8b)$$

For the case of full response systems ( $L=1$ ),  $S$  corresponds to the number of physical phase states. The number of phase transitions is therefore  $\Xi=S \cdot M$ . For this reason the number of  $2\Xi$  filters becomes intolerable for high  $M$  and/or weak  $h$ .

Each transition has the incremental metric

$$\Lambda_i(b) = \|y(t, \gamma_i) - \tau_b(t)\|^2 = \|y(t, \gamma_i)\|^2 + \|\tau_b(t)\|^2 - 2\langle y(t, \gamma_i), \tau_b(t) \rangle \quad (9)$$

As a result, MLSD must search for the sequence having maximum cumulative metric given by the inner product

$$\Lambda_i(b) = \langle y(t, \gamma_i), \tau_b(t) \rangle. \quad (10)$$

## III. RECEIVER STRUCTURE

Initially, the bank of matched filters is replaced by a system of projections into a signal space resulting from the spanning of very few Walsh functions [3]. Afterwards, a processor calculates metrics using matrix algebra [4, 5]. The second simplification is made on the metrics calculation block for each channel symbol. It is applied an algorithm and a data structure that, jointly, consent to obtain all the metrics keeping in memory only 1/8 of the phase transitions, and allow to obtain their total number from just 1/4 of the metrics [6]. The method is valid for a subclass of CPM schemes (which comprehend the best ones), where phase transitions have certain symmetry

relations that can be translated to relations between positions on a table. Finally, MLSD is made with the M-algorithm. The receiver structure is depicted in Fig. 1.

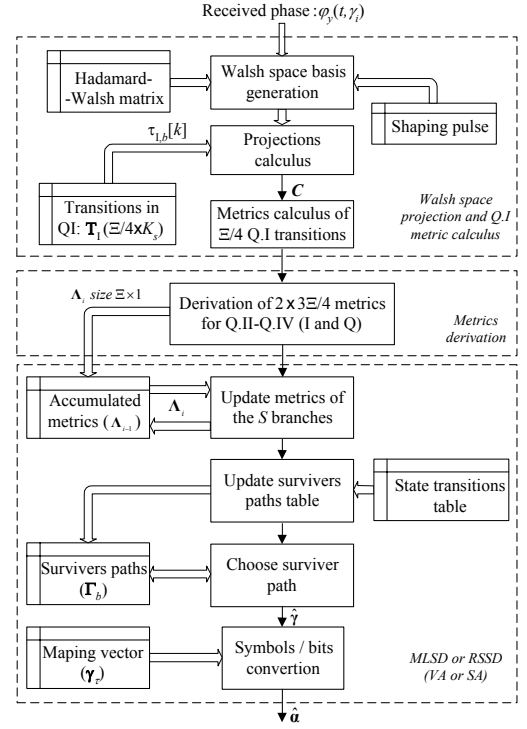


Figure 1. Structure of the proposed receiver.

### A. Projections and calculus of $I^{\text{st}}$ quadrant metric

Metrics are calculated on a  $F$ -dimensional Walsh space, generated by  $F$  Walsh functions [3] of order  $k$  denoted as  $w_{F,n}(t)$ ;  $n=1, 2, 3, \dots, F=2^k$ , each one with  $F=2^k$  symbols, being them  $w_{F,n}[j]$ ,  $j=0, 1, \dots, F=2^k$ , for  $k \in \mathbb{Z}^+$ :

$$\tilde{w}_{F,n}(t) = \frac{1}{\sqrt{T_s}} \sum_{j=0}^{F-1} w_{F,n}[j] \cdot \text{rect}\left[\frac{t - (T_s/(2F)) - j(T_s/F)}{T_s/F}\right] \quad (11)$$

with  $n=0, 1, \dots, F-1=2^u-1$ ,  $u \in \mathbb{Z}^+$ , and  $\text{rect}(t)=1$  for  $|t| < 1/2$  and zero elsewhere. Symbols  $w_{F,n}[j] \in \{-1, +1\}$  and are defined by a recursive method that builds *Walsh-Hadamard matrixes* [3]. Generalizing (3) it can be proved that the  $b^{\text{th}}$  metric in the Walsh space when applying a MLSD criterion is given by

$$\Lambda_i(b) = \left[ \sum_{n=1}^F \int_{iT_i}^{(i+1)T_i} y(t) \cdot \tilde{w}_{F,n}(t) dt - \int_{iT_i}^{(i+1)T_i} s(t, \gamma_b) \cdot \tilde{w}_{F,n}(t) dt \right]^2 \quad (12)$$

for  $b=1, 2, \dots, \Xi$ . Metric calculus is made merely using the projection of the received baseband signal  $y(t)$  into the Walsh space. Those projections coefficients are

$$c_{i,n} = \frac{1}{\sqrt{T_s}} \int_{iT_i}^{(i+1)T_i} y(t, \gamma_i) \cdot w_{F,n}(t - iT_s) dt \quad (13)$$

From (12), the transitions metrics are

$$\Lambda_i(b) = \frac{1}{\sqrt{T_s}} \sum_{n=1}^F |c_{i,n} - c_{b,n}|^2, \quad \text{for } b=1, 2, \dots, \Xi, \quad (14)$$

where  $c_{i,n}$  are the projection coefficients of the transition during symbol interval  $i$ , as given by (13), and  $c_{b,n}$  are projection coefficients of the  $b^{\text{th}}$  transition belonging to the set of  $\Xi$  possible ones. Using the projection vectors and (10), it comes

$$\Lambda_i(b) = \frac{1}{\sqrt{T_s}} \sum_{n=1}^F c_{i,n} c_{b,n}, \quad b=1, 2, \dots, \Xi. \quad (15)$$

These coefficients can be easily determined by:

$$c_{i,n} = \frac{1}{\sqrt{T_s}} \sum_{j=0}^{F-1} w_{F,n}[j] \cdot \int_{(i+j/F)T_s}^{(i+(j+1)/F)T_s} y(t, \gamma_i) dt. \quad (16)$$

Moreover, each integrator does not need to be dumped at every  $T_s/F$  sub-interval. By sampling the continuous integration it is possible to know the partial integration values making

$$c_{i,n} = \frac{1}{\sqrt{T_s}} \sum_{j=1}^F w_{F,n}[j] \left[ \left( \int_{iT_s}^t y(t, \gamma_i) dt \right) \Big|_{t=j\frac{T_s}{F}} - \left( \int_{iT_s}^t y(t, \gamma_i) dt \right) \Big|_{t=(j-1)\frac{T_s}{F}} \right], \quad iT_s < t < (i+1)T_s. \quad (17)$$

The calculation on (17) only requires two integrators, a sampling procedure and a calculus unit [5], independently of the CPM scheme.

The vector of  $\Xi$  metrics is the column vector

$$\Lambda_i = [d_i^2(1) \ d_i^2(2) \ \dots \ d_i^2(b) \ d_i^2(b+1) \ \dots \ d_i^2(\Xi)]^T. \quad (18)$$

The received  $i^{\text{th}}$  transition has a description on the Walsh space given by the projection vector

$$\mathbf{c}_i = [c_{i,1} \ c_{i,2} \ \dots \ c_{i,n} \ \dots \ c_{i,F}] \quad , \quad i=1, 2, \dots, N_s. \quad (19)$$

Each possible transitions is stored on on similar vectors:

$$\mathbf{c}_b = [c_{b,1} \ c_{b,2} \ \dots \ c_{b,n} \ \dots \ c_{b,F}] \quad , \quad b=1, 2, \dots, \Xi. \quad (20)$$

Coefficients,  $c_{b,n}$ , can be determined and memorized in advance. Vectors  $\mathbf{c}_b$  can form matrix  $\mathbf{C}$  of dimensions  $\Xi \times F$

$$\mathbf{C} = \begin{bmatrix} \mathbf{c}_1 \\ \mathbf{c}_2 \\ \vdots \\ \mathbf{c}_b \\ \vdots \\ \mathbf{c}_{\Xi} \end{bmatrix} = \begin{bmatrix} c_{1,1} & c_{1,2} & \dots & c_{1,n} & \dots & c_{1,F} \\ c_{2,1} & c_{2,2} & \dots & c_{2,n} & \dots & c_{2,F} \\ \vdots & \vdots & \vdots & \vdots & \vdots & \vdots \\ c_{b,1} & c_{b,2} & \dots & c_{b,n} & \dots & c_{b,F} \\ \vdots & \vdots & \vdots & \vdots & \vdots & \vdots \\ c_{\Xi,1} & c_{\Xi,2} & \dots & c_{\Xi,n} & \dots & c_{\Xi,F} \end{bmatrix}. \quad (21)$$

Having  $\mathbf{C}$ , the incremental distance vector (metrics) is

$$\Lambda_i = \begin{bmatrix} d_i^2(1) \\ d_i^2(2) \\ \vdots \\ d_i^2(b) \\ \vdots \\ d_i^2(\Xi) \end{bmatrix} = \begin{bmatrix} c_{1,1} & c_{1,2} & \dots & c_{1,n} & \dots & c_{1,F} \\ c_{2,1} & c_{2,2} & \dots & c_{2,n} & \dots & c_{2,F} \\ \vdots & \vdots & \vdots & \vdots & \vdots & \vdots \\ c_{b,1} & c_{b,2} & \dots & c_{b,n} & \dots & c_{b,F} \\ \vdots & \vdots & \vdots & \vdots & \vdots & \vdots \\ c_{\Xi,1} & c_{\Xi,2} & \dots & c_{\Xi,n} & \dots & c_{\Xi,F} \end{bmatrix} \begin{bmatrix} c_{i,1} \\ c_{i,2} \\ \vdots \\ c_{i,n} \\ \vdots \\ c_{i,F} \end{bmatrix}$$

$$= \mathbf{C} \cdot \mathbf{c}_i^T \quad , \quad i=1, 2, \dots, N_s. \quad (22)$$

conducting to the intended column vector with the metrics.

## B. Metric derivations

By restraining CPM schemes to those having a number of states  $S \equiv 0 \pmod{4}$  ( $S \geq 4$ ), one can reduce memory size and the number of operations. Only transitions metrics associated to transitions emerging from first quadrant must be calculated, and only for the *in phase* branch. All the others metrics (other quadrants and Q ones) are related to them, substituting integral operations by simple copy and paste of real numbers. For that class of schemes we can always distribute the states by the four quadrants in a symmetric manner (Fig. 2), placing  $q/2$  states inside each quadrant. In Fig. 2 it is analyzed a case of a transition  $\tau_b$  in quadrant I. It's possible to see that the *in phase* transition,  $\tau_{1,b}$ , is the equal to the one of  $\tau_b$  in quadrant IV and symmetric of  $\tau_b$ . Observations of this type are also illustrated for the Q branch. The channel symbols  $\gamma_m$  form the vector  $\boldsymbol{\gamma} = \{\gamma_1, \gamma_2, \dots, \gamma_M\}$ . Notation such as  $\tau(\gamma_\tau[m])$  refers to a phase transition associated to the symbol of the vector in position  $m$ .  $\tau(\gamma_b)$  denotes exactly the same in a shorter way, being  $m=b - (M \times (\text{"state \#"} - 1))$ . For states number  $n_1=1, 2, \dots, S$ , inside quadrants I, II, III and IV, the procedure to obtain all the metrics  $\Lambda_b$ , using the specified data structures, should be:

- Q.I: calculate the metrics for each  $M$  transition initiating in each state inside the quadrant I. For each  $\mathbf{T}[b=n_1+n_2, k] = \tau(\gamma_\tau[n_2])$ , for  $n_2=1, 2, \dots, M$ , calculate:

$$d_{1,b}^2 = \mathbf{y}_i \cdot (\boldsymbol{\tau}_{1,b})^T = \sum_{k=1}^{K_s} y[k - iK_s] \cdot \cos(\tau_b[k]) \quad (23a)$$

$$d_{Q,b}^2 = \mathbf{y}_i \cdot (\boldsymbol{\tau}_{Q,b})^T = \sum_{k=1}^{K_s} y[k - iK_s] \cdot \sin(\tau_b[k]). \quad (23b)$$

One can also remember that phase transitions and its sine and cosine functions are related by  $\sin(\varphi) = \cos(\varphi - \pi/2)$ . For that reason matrix  $\mathbf{T}_Q$ , containing the transitions signals in quadrature, does not need to be stored. Those transitions already exist inside matrix  $\mathbf{T}_I$ , each one located precisely  $q/2 \cdot M$  positions before, considering mod  $\Xi$  operations. So (24b) can be applied using:

$$d_{Q,b}^2 \mathbf{y}_i \cdot \left( \boldsymbol{\tau}_{1,b - \frac{q}{2}M \pmod{\Xi/4}} \right)^T = \sum_{k=1}^{K_s} y[k - iK_s] \cdot \cos\left( \tau_{b - \frac{q}{2}M \pmod{\Xi/4}}[k] \right). \quad (24)$$

Up until now,  $\Xi/4$  metrics have been successively calculated and placed inside  $\Lambda$  in positions  $b_1 = n_1 + n_2$ . States  $S^{(n_1)}$  are associated to  $n_1=1, 2, \dots, S/4$  and transitions to  $n_2=1, 2, \dots, M$ . Metrics for quadrants II, III and IV will be copied from them in the following manner:

- Q.II: Metrics associated to transitions initiating in states  $S^{(q-n_1)}$  are copied from positions  $b_1$  to positions  $b_{II}$  for the symmetric symbol of  $\boldsymbol{\gamma}_\tau$  (due to the inverse rotations exposed in Fig. 2) respecting  $d_{1,b}^2 = -d_{1,b}^2$  ;  $d_{Q,b}^2 = d_{Q,b}^2$  ;  $b_{II} = (q-n_1)M + (M-n_2)$ .

#### IV. TEST SCHEMES, CHANNEL AND RECEIVER

In order to research the behaviour of the receiver we have used the  $h=1/2$  full response  $M$ -ary schemes presented in Table 1 (MSK on the first line), taking advantage of their very low number of states ( $S=4$ ). Those simple schemes happen to be catastrophic, that is, their MNSED has a local mean for the used  $h=1/2$ , being the real  $d_{\min}^2$  very distant from its upper bound [2]. That concerns only to the MLSD block and should not influence the research on the metric calculus using the CPM space approximation. From [2,5,9,10] we point out two optimum full response mono- $h$  CPM schemes also characterized on Table 1.

Table 1: Characteristics of 1REC CPM schemes (gain evaluation for channels with AWGN)

$h$	$M$	$S$	$B_{99,0}T_b$	$d_{\min}^2$	$G$ [dB]	$\Xi$	$2\Xi$
1/2	2	4	1.20	2.0	0	8	16
	4	4	1.30	2.0	0	16	32
	8	4	1.55	3.0	1.76	32	64
	16	4	N.A.	4.0	3.0	64	128
9/20	4	40	1.18	3.60	2.56	160	320
	8	40	1.40	5.40	4.31	320	640

The selected schemes of  $h=0.45=9/20$  are the best 4-ary and 8-ary CPFSK schemes in terms of power gains within the region of useful spectral efficiencies which preserve an acceptable number of states ( $S=40$ ). These two schemes of  $h=0.45$  share another interesting feature: they are precisely examples of rare schemes with a MNSED coincident with their upper bound curves (determined by simulation in [1,2]).

In narrow-band wireless systems the signal is received with AWGN and a multiplicative distortion (frequency-flat Rayleigh fading – FFRF). The latter is obtained by means of two independent gaussian processes ( $n_x, n_y$ ), being

$$y(t, \boldsymbol{\gamma}) = R(t) \cdot s(t, \boldsymbol{\gamma}) + n(t) = \sqrt{n_x^2 + n_y^2} \cdot s(t, \boldsymbol{\gamma}) + n(t). \quad (28)$$

The classical Doppler filtering of the Rayleigh process  $R(t)$  was applied, considering a scenario with a carrier on 1 GHz, a relative velocity of  $v=50$  km/h among transmitter and receiver, and a bit rate of 312.5 kbit/s. This conducts to a maximum frequency deviation for the Doppler spectrum of  $f_{\max} = v/\lambda = 46.3$  Hz ( $\lambda$  being the carrier wavelength). The random phase shift introduced by this type of fading is uniformly distributed, being  $\Delta\phi \in [-\pi, +\pi]$ . In general it is a straightforward process to estimate the FFRF channel phase response, thus, it can be compensated. In our simulation for the  $h=1/2$  schemes we consider the two extreme cases: no phase compensation and total phase compensation, thereby emulating ideal coherent demodulation. For the  $h=9/20$  schemes, the interesting ones, the proposed receivers are assessed considering an error phase limited to 10%, i.e.  $\Delta\phi \in [-0.1\pi, +0.1\pi]$ , jointly with those extreme cases of phase synchronism. Though, amplitude fading is never compensated.

From [4, 5] it is known that for all tested schemes a number of Walsh functions equal to  $M$  ( $F=M$ ) assures near optimum performance. For higher Walsh space dimensions ( $F>M$ ) no significant gains are detected. A  $F<M$  implies an abrupt decay

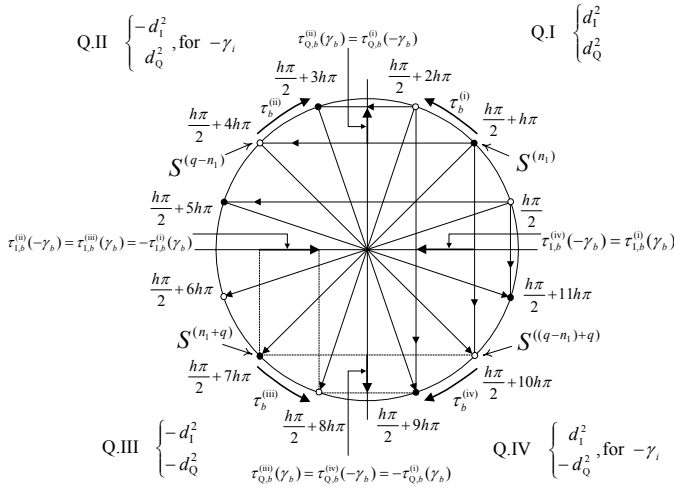


Figure 2: Metric relations and coping procedures (example for  $h=1/6$ ,  $S=12$ )

- Q.III: For states  $S^{((q-n_1)+q)}$ , metrics should be copied from  $b_I$  to positions  $b_{III}$  respecting  $d_{1,b}^2 = -d_{1,b}^2$ ;  $d_{Q,b}^2 = -d_{Q,b}^2$ ;  $b_{III} = b_{II} + q = n_1 + n_2 + qM$ .

- Q.IV: For the states  $S^{((q-n_1)+q)}$ , metrics should be copied from  $b_I$  to positions  $b_{IV}$  respecting  $d_{1,b}^2 = d_{1,b}^2$ ;  $d_{Q,b}^2 = -d_{Q,b}^2$ ;  $b_{IV} = b_{II} + q = (q-n_1)M + (M-n_2) + qM$ .

In all cases  $n_2$  always runs the cycle  $n_2=1, 2, \dots, M$ . Metrics are copied and pasted between positions on a table by this manner, affected by “ $\pm$ ” signals depending on quadrants and if it’s a  $\Lambda_{1,b}$  or  $\Lambda_{Q,b}$  metric. The final vector of  $\Xi$  metrics,  $\mathbf{\Lambda}_s$ , stores the sums of those partial metrics.

#### C. Complexity constrained MLSD

Having all the metrics the problem remains on search of the most probable sequence of phase transitions. For that purpose the Viterbi Algorithm (VA) is widely used. It performs maximum likelihood sequence detection (MLSD) but its complexity can limit its use [7]. Complexity constrained MLSD can be described by the *search algorithm*, which separates the  $S$  states into  $C$  classes. Hence, every class contains  $S/C$  states. Within each class some paths are discarded at each symbol decision.  $B$  is the number of paths chosen to remain in competition inside each class. This algorithm and its variables are denoted by  $SA(B, C)$ . One can recognize the VA as being the particular case  $SA(1, S)$ . The entire  $SA(B, C)$  family performs MLSD [8]. Whenever one search is conducted inside partitions the algorithm is usually named reduced state sequence detection (RSSD). RSSD can be denoted by  $SA(1, C)$ . At the beginning of each interval  $MB$  transitions emerge, but only  $N_p=BC$  paths are stored as initial states of the next iteration and  $N_p$  is always  $<S$ . So,  $SA(B=N_p, 1)$  conducts to the best performance since it is the least constrained situation. The  $M$ -algorithm corresponds to the  $SA(B, 1)$ , being  $M=B$ . This is the algorithm implemented on the receiver due to its simplicity and for belonging to the family of best performance. In the limit of  $B=1$  one gets decision feedback (DF), i.e.,  $SA(1, 1)$ ; only one path is traced for the sequence detection. It corresponds to the case of less computational weight but the probability of losing the correct path is the highest one.

of performance. This rule also applies to the interesting schemes of  $h=9/20$ : in AWGN one gets for  $M=8$  with  $F=8$  a BER curve as close as 0.2 dB from the optimum detection curve and for  $M=4$  with  $F=4$  the power loss is less than 0.1 dB. Consequently, in this paper we tested the same receivers [5]. In [11] it was seen that a 10% phase estimation virtually introduces no error on the detection. For that reason, that is the standard used for testing the receiver during this research. It was also proved in [11] that in AWGN the M-algorithm can assure quasi-optimum performance for a number B of paths in the trellis as low as the M-arity. So the proposed receivers are all defined with  $B=M=F$ .

## V. RESULTS

Results for performance in terms of bit error rate (BER) are given in both Figures 3 and 4. Both figures include the BER curve for ideal antipodal modulation ( $d_{\min}^2 = 2$ ) and the BER curve associated to  $d_{\min}^2 = 1.7$ , which was proposed by [12] to describe real MSK, both for AWGN. On Figure 4 the curve for the proposed receiver for MSK is repeated from Figure 3 for a better comparison of the three proposed schemes and associated receivers: quaternary and octonary 1REC  $h=9/20$  and MSK, using receivers defined by the rules given above.

The proposed MSK receiver presents a power loss of 1.5 dB to the optimum receiver (optimum on AWGN) with perfect phase estimation. It can be seen that, over the FFRF channel, an increase on modulation complexity does not imply such a fast increase in  $G$  as on AWGN. For example, for  $h=1/2$ ,  $M=8$  or  $M=16$  conduct to the same  $G \approx 3$  dB to the MSK curve. The  $h=9/20$  schemes exhibit over FFRF less significant gains to MSK than the ones found only with AWGN. The proposed receivers show a power loss of  $\approx 2$ dB to the corresponding optimum receiver with coherent demodulation (with phase estimation and compensation).

## VI. CONCLUSIONS

A CPM receiver with high complexity reduction at all detection stages proved to be robust in terms of phase failures over frequency-flat Rayleigh fading. The rules previously found with AWGN, which defined limits for the receiver parameters in terms of Walsh functions and number of states in the M-Algorithm, proved to achieve almost the same results with the fading environment for some test schemes and as well for interesting high gain schemes. Near-optimum performance was attained when using a receiver with a front-end based on a Walsh of dimension as small as the M-arity and propagating the same number of paths in the trellis. In addition, the metric derivation algorithm is found to be robust when dealing with phase errors introduced by the considered fading.

## REFERENCES

- [1] J. Anderson, T. Aulin, C. Sundberg, *Digital Phase Modulation*, Plenum Press, New York, 1986.
- [2] T. Aulin and C-E. Sundberg, "Continuous Phase Modulation - Part I: Full Response Signalling", *IEEE Trans. on Comm.*, vol. Com-29, no. 3, pp. 196-209, Mar. 1981.
- [3] L. E. Franks, *Signal Theory*, Prentice-Hall, 1969.

- [4] Weiyi Tang and Ed Shweddyk, "A Quasi-Optimum Receiver for Continuous Phase Modulation", *IEEE Trans. on Comm*, vol. 48, no. 7, pp. 1087-1090, July 2000.
- [5] F. Monteiro and A. Rodrigues, "Limits for CPM Signals Representation by Walsh Functions", unpublished.
- [6] F. Monteiro and A. Rodrigues, "Simple Metrics Derivation for a Discrete Time Continuous Phase Modulations Receiver", in *Proc. WPMC'01 - 4th Inter. Symp. on Wireless Personal Multimedia Comm.*, Aalborg, Denmark, pp. 395-400, Sept. 2001.
- [7] J. Hayes, "The Viterbi Algorithm Applied to Digital Data Transmission", *IEEE Comm. Mag.*, 50<sup>th</sup> Anniversary Commemorative Issue, pp. 26-32, May 2002.
- [8] T. Aulin, "Breadth-First Maximum Likelihood Sequence Detection", *IEEE Transactions on Communications*, vol. 47, no. 2, pp. 208-216, Feb. 1999.
- [9] T. Aulin and C-E Sundberg, "Minimum Euclidean Distance and Power Spectrum for a Class of Smoothed Phase Modulation-Codes with Constant Envelope", *IEEE Transactions on Communications*, vol. Com-30, no. 7, pp. 1721-1729, July 1982.
- [10] I. Sasase and S. Mori, "Multi- $h$  Phase-Coded Modulation", *IEEE Com. Mag.*, vol. 29, no. 12, pp. 46-56, Dec. 1991.
- [11] F. Monteiro, *Complexity Reduction of CPM Receivers for Wireless Communications Systems*, M.Sc. thesis (in Portuguese), IST - Technical University of Lisbon, Portugal, Jan. 2003.
- [12] Z. Murota and K. Hirade, "GMSK Modulation for Digital Mobile Radio Telephony", *IEEE Trans. on Comm.*, vol. Com-29, no. 7, July 1981.

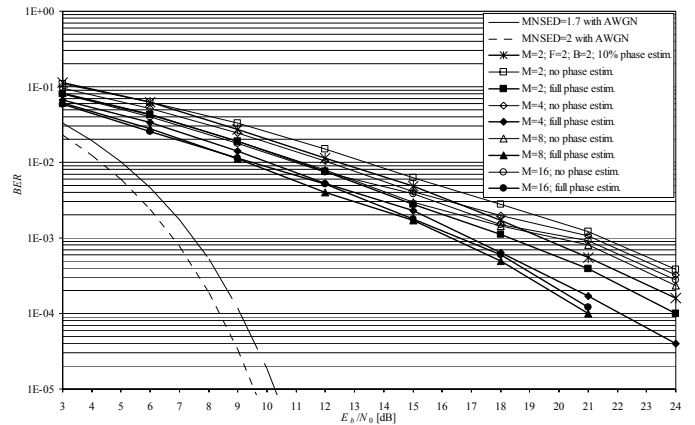


Figure 3: Effect of the phase estimation on the optimum receiver (with matched filters and Viterbi detection) when operating with the metrics derivation algorithm for the schemes having  $h=1/2$ .

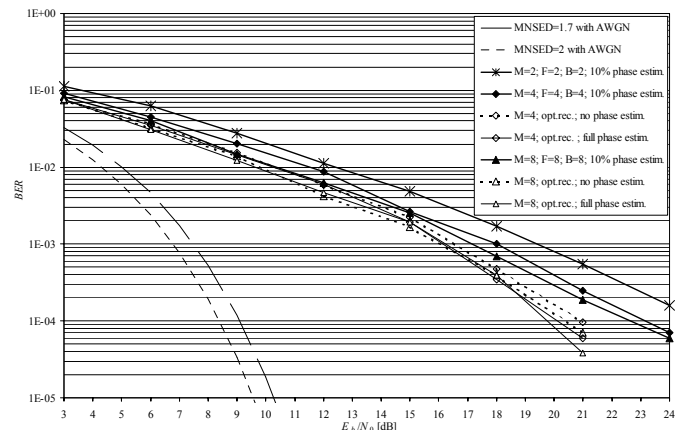


Figure 4: Comparison of reduced complexity receivers and optimum receivers with and without phase compensation for the optimum  $h=9/20$  schemes.